



On the relationship between eastern China aerosols and western North Pacific tropical cyclone activity



Haikun Zhao^{a,*}, Yunjie Jiang^a, Kai Zhao^a, Jian Cao^a, Philip J. Klotzbach^b, Graciela B. Raga^c, Liguang Wu^d

^a Key Laboratory of Meteorological Disaster, Ministry of Education, and Joint International Research Laboratory of Climate and Environment Change, and Collaborative Innovation Center on Forecast and Evaluation of Meteorological Disaster, and Pacific Typhoon Research Center, Nanjing University of Information Science and Technology, Nanjing, China

^b Department of Atmospheric Science, Colorado State University, Fort Collins, CO, USA

^c Instituto de Ciencias de la Atmósfera y Cambio Climático, Universidad Nacional Autónoma de México, Mexico City, Mexico

^d Department of Atmospheric and Oceanic Sciences and Institute of Atmospheric Sciences, Fudan University, Shanghai, China

ARTICLE INFO

Keywords:

Tropical cyclones
Eastern China aerosols
Pacific Meridional Mode
Typhoons

ABSTRACT

How aerosols affect the weather and climate system has received increasing attention. This study finds a significant negative correlation between March–May eastern China aerosol optical depth (AOD) and July–November western North Pacific (WNP) tropical cyclone (TC) frequency during 2003–2020. This time period spans when several aerosol reanalyses are available and both Terra and Aqua Moderate Resolution Imaging Spectroradiometer AOD retrievals are assimilated therein. Composite analyses and budget analyses of dynamical genesis potential indices indicate the importance of large-scale environmental factors, especially vertical velocity and vertical wind shear, associated with changes in AOD that in turn modulate changes in WNP TC frequency. Increased eastern China AOD may facilitate negative Pacific meridional mode development via modulation of the westerly jet, which then forces an anticyclonic circulation over the WNP basin. Increased AOD can also directly decrease the inter-hemispheric temperature differential and increases the intra-hemispheric temperature differential between the equator and the mid-latitudes, thus weakening ascending motion and enhancing vertical wind shear over the WNP, especially the southeastern portion of the basin. All of these large-scale environment changes induced by increased eastern China AOD tend to suppress WNP TCs. This study highlights the potential influence of eastern China aerosol loadings on WNP TCs, thus improving our understanding of TC climate variability over the WNP.

1. Introduction

Tropical cyclones (TCs) can cause significant coastal impacts due to wind, rainfall and storm surge (Peduzzi et al., 2012; Eberenz et al., 2021; Zhao et al., 2022a). In a warming environment, TC-associated damage appears to show an increasing trend with projected increases in TC intensity, precipitation, and accompanying storm surges and floods (Chan and Liu, 2004; Y. Sun et al., 2017; Knutson et al., 2020; Yamaguchi et al., 2020). While there is uncertainty about whether TC frequency will change in the future, there is a general consensus that TC intensity will increase with global warming (Knutson et al., 2020; Zhao et al., 2022b).

Atmospheric aerosols, one of the leading climate forcings, can partly offset greenhouse gases-induced warming via atmospheric cooling

(Kiehl and Briegleb, 1993; Seong et al., 2021). There has been an increasing focus in recent years in estimating the impact of aerosols at various time scales, from synoptic to climate scales (Lohmann and Feichter, 2005; Quaas et al., 2008; Persad and Caldeira, 2018). Aerosols significantly modulate cloud microphysics and thus latent heat release rates, dynamics, and precipitation (Levin and Cotton, 2008; Khain et al., 2009; Rosenfeld et al., 2008). Small aerosols may increase updrafts and cloud top height in deep convective clouds (Khain et al., 2004, 2005, 2008a, 2008b; Koren et al., 2005; Lynn et al., 2005; Wang, 2005; Lee et al., 2008; Khain, 2009). Observational studies have further found that aerosols may impact TC development through their influence on cloud microphysics (Jenkins et al., 2008; Jenkins and Pratt, 2008). The indirect effect of latent heat modulation caused by aerosols may modify TC

* Corresponding author at: Nanjing University of Information Science and Technology, China.

E-mail addresses: haikunzhao@nuist.edu.cn (H. Zhao), jianc@nuist.edu.cn (J. Cao).

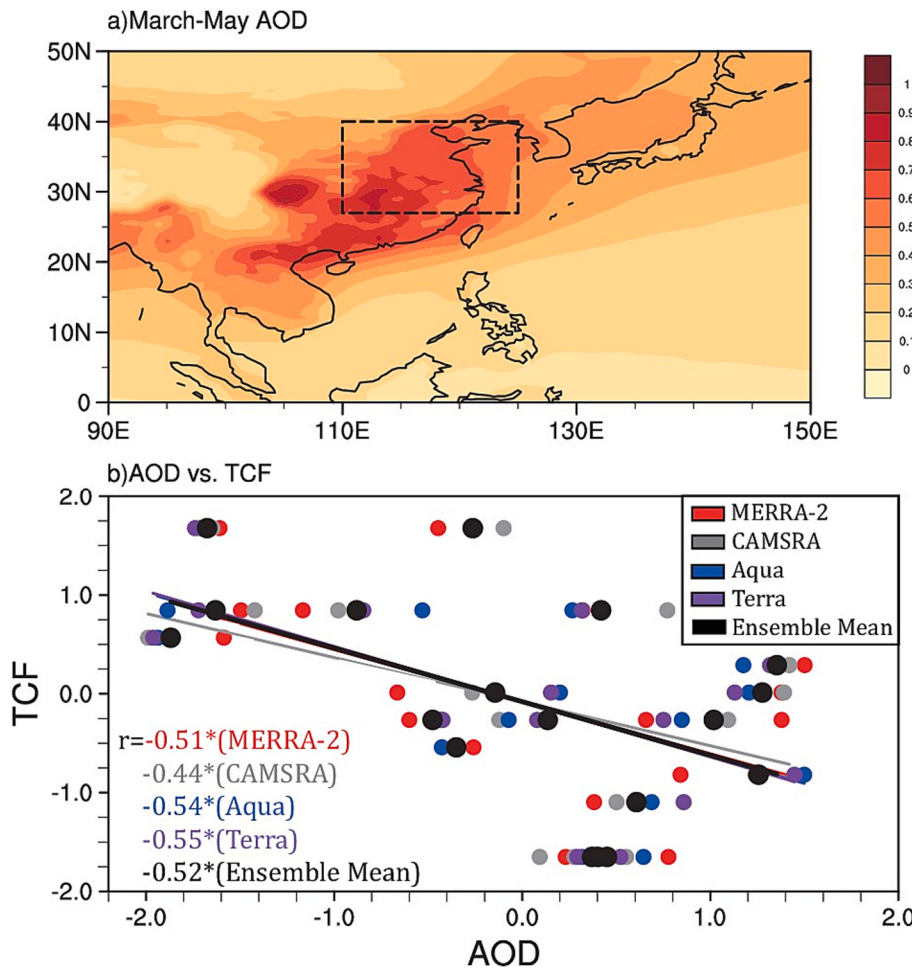


Fig. 1. (a) Climatological distribution of March–May averaged aerosol optical depth (AOD) from 2003 to 2020. The location of the eastern China AOD region [27°N–40°N, 110°E–125°E] is denoted by the black dashed rectangle. (b) Standardized time series of March–May averaged AOD over eastern China from MERRA-2, CAMSRA, MODIS Aqua and Terra products as well as the ensemble mean of these four datasets and July–November western North Pacific tropical cyclone frequency (TCF) during 2003–2020. Correlation coefficients that are statistically significant are denoted with an “*”. (For interpretation of the references to colour in this figure legend, the reader is referred to the web version of this article.)

size and intensity (Khain et al., 2005; van den Heever et al., 2006). Wang et al. (2014) also suggested that increased storm intensity and decreased storm size may occur in response to increased aerosol concentration. TC-aerosol interactions can furthermore substantially affect the prediction errors of TC intensity (Rosenfeld et al., 2011).

Several studies have examined the impact of anthropogenic aerosols on both individual TC basin frequency and global TC frequency on long-term time scales (Mann and Emanuel, 2006; Dunstone et al., 2013; Takahashi et al., 2017; Chiacchio et al., 2017; Cao et al., 2021, 2022a). Aerosols can cool sea surface temperatures, thus changing the frequency and intensity of ENSO events (McGregor and Timmermann, 2011; Maher et al., 2015; Khodri et al., 2017; Pausata et al., 2016) and their associated modulation of the large-scale TC environment. Pausata and Camargo (2019) suggested that aerosols caused by large volcanic eruptions can cause shifts in the intertropical convergence zone, thus redistributing global TC activity. Cao et al. (2021) found that anthropogenic aerosol emissions can cause an asymmetric distribution of TCs, with reduced Northern Hemisphere TCs and increased Southern Hemisphere TCs, primarily through alterations in vertical wind shear and mid-tropospheric vertical motion. Anthropogenic aerosols cool the Northern Hemisphere relative to the Southern Hemisphere, resulting in stronger meridional temperature gradients between the equator and mid-latitudes in the Northern Hemisphere and weaker meridional temperature gradients between the equator and mid-latitudes in the Southern Hemisphere (Cao et al., 2021, 2022a).

Non-uniform aerosol distributions can exert distinct impacts on regional circulations and thus, on regional TC activity (Liu et al., 2010; Jones et al., 2017; Stevens et al., 2017; Persad et al., 2018). Over the western North Pacific (WNP) basin, TC activity has significantly trended

downward over the past 20 years (Liu and Chan, 2013; Takahashi et al., 2017). Several recent studies have focused on the importance of the tropical Pacific climate shift and shifting ENSO conditions on the decreasing trend (Chan, 2008; Lee et al., 2012; Zhao et al., 2019, 2021a, b; Klotzbach et al., 2022). Other studies have emphasized the potential impact of aerosols. Takahashi et al. (2017) demonstrated an important role of aerosols in the downward trend of WNP TC activity, especially over the southeast portion of the basin. They found that these decreases were due to increased vertical wind shear and reduced low-level vorticity, driven by aerosol-modulated changes of sea surface temperature anomalies (SSTAs).

The impact of aerosols on seasonal and longer time scales has been relatively less studied. Xian et al. (2020) found a significant negative correlation between African dust aerosol optical depth (AOD) and Atlantic TCs in summer and further pointed out that African dust AOD can exert impacts on the Atlantic meridional mode, thus changing the associated large-scale fields affecting TCs. Other studies have investigated the impact of regional aerosol concentrations on regional climate (Ramanathan et al., 2001; Zhao et al., 2006; Tie and Cao, 2009). Accompanied by rapid economic development over the past several decades, aerosols over eastern China have significantly increased, impacting both local and regional climate (Tie et al., 2006; Chen et al., 2020). During recent decades, light rainfall frequency has decreased throughout eastern China. The indirect effect of aerosols has been implicated as a potential reason for the observed decrease in light rainfall (Choi et al., 2008; Qian et al., 2009). Given the impact of aerosol cooling on the meridional circulation and the land-sea thermal contrast, large-scale atmospheric and oceanic circulations also change (Gu et al., 2006; Wu et al., 2016; Cao et al., 2022b). Since aerosols have short

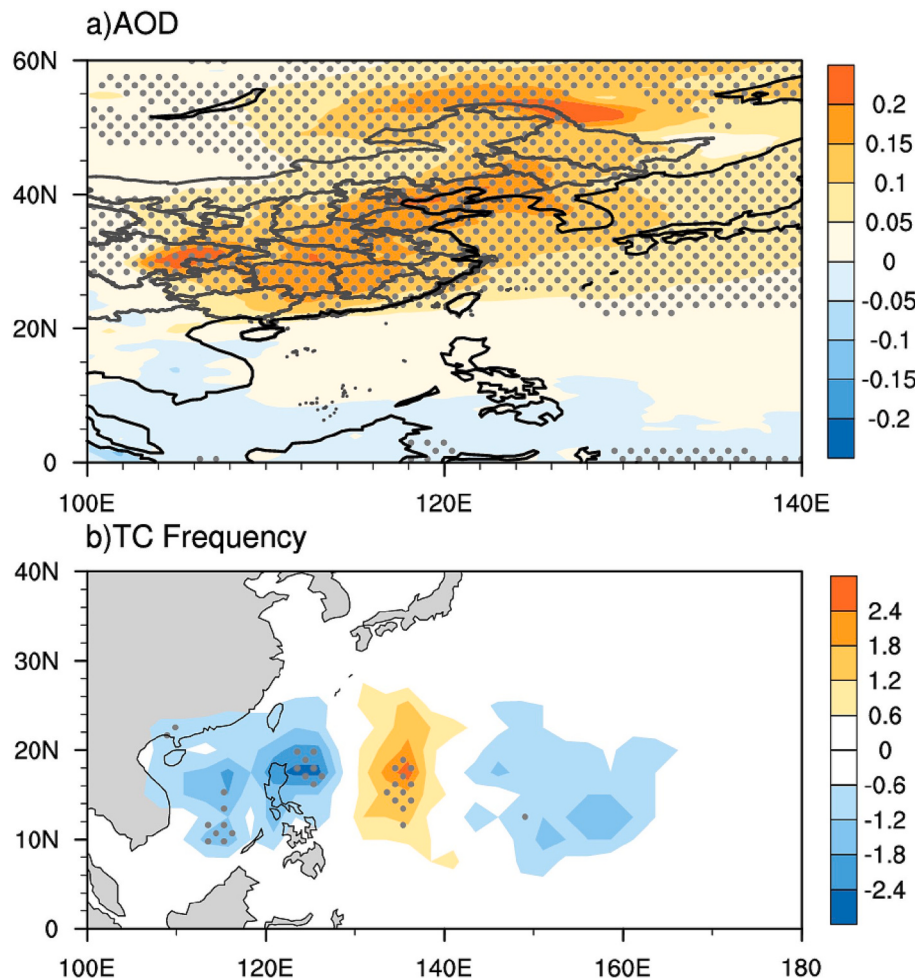


Fig. 2. Difference of (a) March–May AOD and (b) July–November TC frequency between years with the five highest AOD over eastern China (2006, 2007, 2008, 2010, and 2012) and the five years with the lowest AOD over eastern China (2005, 2017, 2018, 2019, and 2020). Grey dots indicate statistically significant values.

lifetimes and a heterogeneous spatial-temporal distribution, there are large uncertainties on quantifying its climate effect (Menon, 2004; Thorsen et al., 2021). Here we attempt to address two questions: Do eastern China aerosols impact peak TC season numbers of WNP TCs? If yes, what is the associated physical mechanism?

The rest of this study is organized as follows. Section 2 describes the methodology and data used. Section 3 highlights the strong relationship between aerosols in eastern China and WNP TCs. Section 4 explores the possible physical mechanisms. A summary is provided in Section 5.

2. Data and methods

2.1. Data

Tropical cyclone data for the WNP from 2003 to 2020 are obtained from the Joint Typhoon Warning Center (JTWC) best track dataset (Chu et al., 2002). This dataset includes TC latitude, longitude, and maximum sustained wind speed at 6-h intervals. In this study, a TC is defined as having maximum sustained wind speeds greater than or equal to 34 kt during the peak TC season from July–November. The TC's genesis location is defined as the location where the TC's winds first reach 34 kt.

Aerosol optical depth data is available from the monthly-averaged AOD analysis based on the Goddard Earth Observing System Earth System Model's Modern-Era Retrospective analysis for Research and Applications, version 2 (MERRA-2) reanalysis (Rienecker et al., 2011) with a horizontal resolution of $0.5^\circ \times 0.625^\circ$ since 1980, Copernicus Atmosphere Monitoring Service reanalysis datasets (CAMSRA) by the

European Centre for Medium Range Weather Forecasts, as well as MODIS Terra and Aqua products since 2003. Although the MERRA-2 aerosol dataset has a longer data record that extends from 1980 to present, MERRA-2 incorporates AOD assimilation from multiple remote sensing sources including AERONET, the Moderate Resolution Imaging Spectroradiometer (MODIS), and Multi-angle Imaging Spectroradiometer satellite products since 2003. This study therefore focuses on the period from 2003 to 2020, when aerosol reanalyses are available and both Terra and Aqua Moderate Resolution Imaging Spectroradiometer (MODIS) AOD retrievals were assimilated therein. All four AOD datasets find a similar significant relationship between spring eastern China AOD peak season WNP TC frequency (discussed in detail in the remainder of this manuscript). Unless otherwise noted, AOD data from MERRA-2 are shown in the following analyses.

Monthly mean atmospheric fields (including relative humidity, 2-m air temperature, wind and vertical velocity) are taken from the monthly NCEP-DOE reanalysis II dataset (Kanamitsu et al., 2002) with a horizontal resolution of $2.5^\circ \times 2.5^\circ$ and 17 vertical pressure levels. Monthly SST data are taken from the National Oceanic and Atmospheric Administration (NOAA) Extended Reconstructed SST version 5 (ERSST v5) with a horizontal resolution of $2.0^\circ \times 2.0^\circ$ (Huang et al., 2015). In this study, we focus on the impact of aerosols on the formation and development of the Pacific meridional mode (PMM) (Chiang and Vimont, 2004). We use the PMM SST index to classify the state of the PMM: <https://www.aos.wisc.edu/~dvimont/MModes/Data.html>.

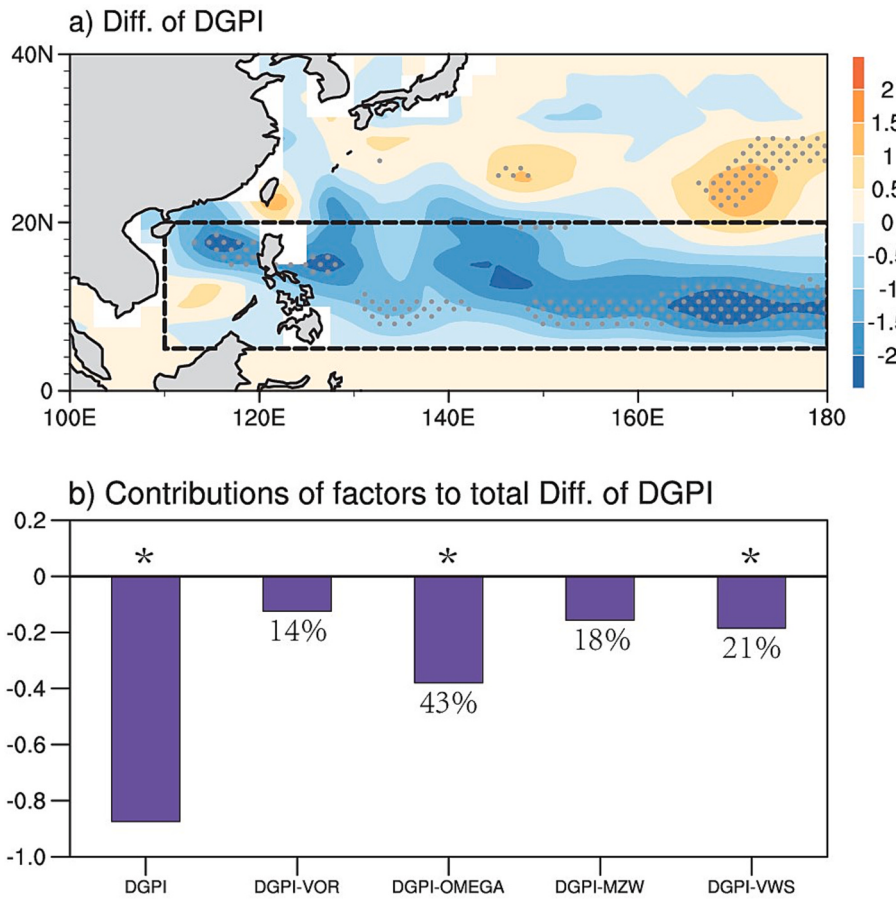


Fig. 3. Difference of the July–November (a) dynamic genesis potential index (DGPI) and (b) Composite difference of total DGPI and DGPI anomalies with the four individually varying factors averaged over [10°N–25°N, 110°E–180°E] between the five years with the highest AOD over eastern China (2006, 2007, 2008, 2010, and 2012) and the five years with the lowest AOD over eastern China (2005, 2017, 2018, 2019, and 2020). The relative contribution of the DGPI anomalies while varying each of the four factors to the total DGPI difference is also displayed in percentage values. Significant composite differences (b) between high AOD and low AOD years are indicated with an “*”.

2.2. Dynamical genesis potential index

To explore the role of large-scale environmental factors on changes in TC genesis frequency, we adopt the dynamic genesis potential index (DGPI) proposed by Wang and Murakami (2020). Murakami and Wang (2022) have shown that the DGPI has a better representation of inter-annual variability of TCs on regional and global scales than the genesis potential index proposed by Emanuel and Nolan (2004). The DGPI is calculated with the following expression:

$$DGPI = (2 + 0.1V_{shear})^{-1.7} \left(5.5 - \frac{\partial u}{\partial y} 10^5 \right)^{2.3} (5 - 20\omega)^{3.3} (5.5 + |10^5 \eta|)^{2.4} e^{-11.8} - 1$$

where V_{shear} represents the vertical wind shear (VWS), calculated as the magnitude of the difference of wind vectors between 200 hPa and 850 hPa, $\frac{\partial u}{\partial y}$ is the 500 hPa meridional gradient of the zonal wind (MZW), ω is the 500 hPa vertical velocity, and η is the 850 hPa absolute vorticity.

In this study, we show that the DGPI can reproduce the distribution of WNP TC genesis, given inter-annual changes of AOD over eastern China. The role of each of the four environmental factors included in the DGPI (e.g., 850 hPa vorticity, 500 hPa ω , 500 hPa MZW and VWS) in controlling inter-annual changes of TC frequency are further assessed, using a similar approach to that used in previous studies (Camargo et al., 2020; Zhao et al., 2018; Cao et al., 2021; Murakami and Wang, 2022; Wang et al., 2021). The total DGPI is calculated with all four variables varying with time. The role of each variable is obtained by keeping one variable varying with time and replacing the other terms with their climatological means. The DGPIs while varying each of the four component variables are respectively referred to as the GPI-VOR, GPI-OMEGA, GPI-MZW, and GPI-VWS, indicating the respective contributions of 850 hPa vorticity, 500 hPa vertical velocity, the meridional

gradient of 500 hPa zonal wind, and vertical wind shear.

2.3. Statistical significance

The statistical significance of correlation coefficients and partial correlation coefficients are tested using a two-tailed Student's *t*-test. *P*-values less than or equal to 0.1 are deemed to be significant.

3. Linkage between eastern China aerosols and WNP TCs

3.1. Relationship between eastern China AOD and WNP TC frequency

During March–May, there is a high concentration of AOD over eastern China (Fig. 1a). March–May AOD over eastern China is 0.58, which is higher than in other seasons (December–February: 0.44; June–August: 0.54; September–October: 0.46). The high concentration of AOD over eastern China in March–May is why we focus on the impact of changes in spring eastern China AOD on WNP TCs in this study. We calculated a timeseries of March–May AOD averaged over eastern China [27°N–40°N, 110°E–125°E] from 2003 to 2020. As shown in Fig. 1b, spring eastern China AOD has a significant negative correlation ($r = -0.51, p < 0.05$) with peak season WNP TC frequency using AOD data from MERRA-2. When AOD data from the other three datasets are used (CAMSRA, Aqua and Terra), we find a similar significant relationship between spring eastern China AOD and peak season TC frequency (Fig. 1b), with correlations of -0.44 for CAMSRA, -0.54 for Aqua, and -0.55 for Terra. The ensemble mean of these four AOD datasets also has a significant correlation ($r = -0.52, p < 0.05$) with peak season TC frequency. These analyses further confirm the robustness of the relationship between eastern China spring AOD and WNP TC frequency from July–November.

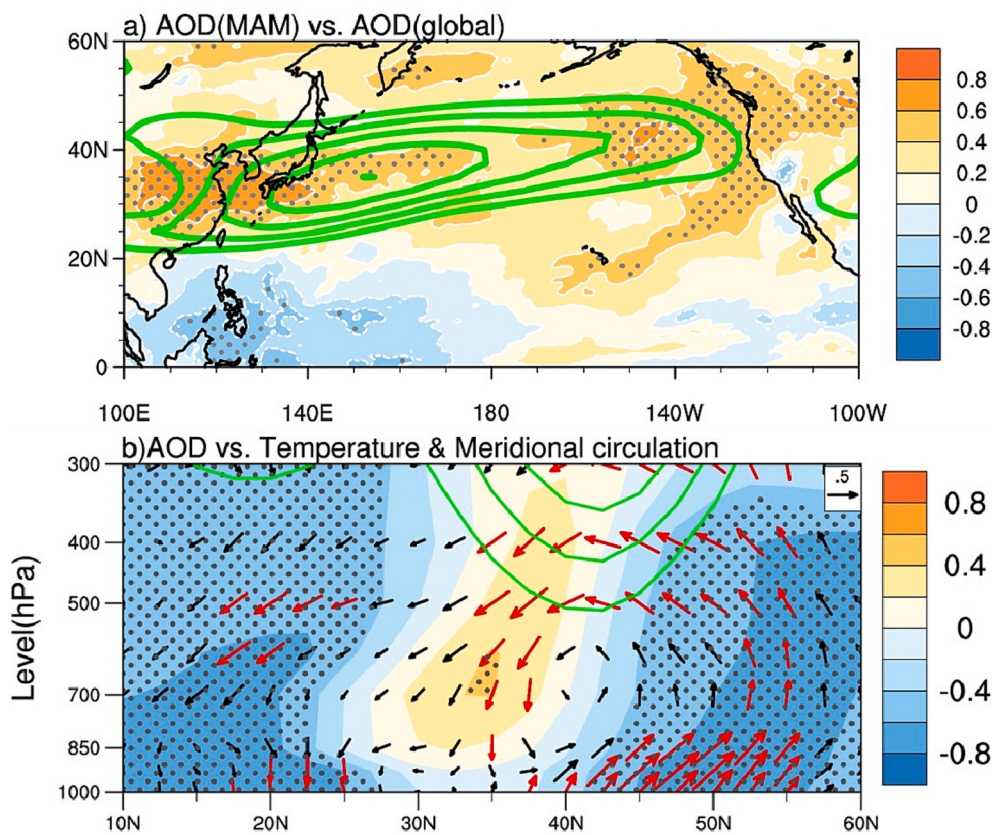


Fig. 4. (a) Correlation map between March–May-averaged eastern China AOD and global AOD during 2003–2020. The green contours represent 500 hPa zonal winds, with an interval of 3 m s⁻¹. (b) Pressure-latitude cross section of March–May eastern China AOD and March–May 2-m air temperature (shading) as well as wind (vectors) averaged over 160°W–120°W. Grey dots and red vectors denote significant correlations. The green contours denote zonal winds, with an interval of 3 m s⁻¹. (For interpretation of the references to colour in this figure legend, the reader is referred to the web version of this article.)

To further investigate eastern China AOD's impact on WNP TCs, the 5 years with the highest AOD over eastern China (2006, 2007, 2008, 2010, and 2012) and the 5 years (2005, 2017, 2018, 2019, and 2020) with the lowest AOD over eastern China during 2003–2020 were selected for composite analyses. As would be expected given the selection criteria, there are significantly higher aerosols in high AOD years over eastern China than during low AOD years (Fig. 2a). Total WNP TC frequency during high AOD years (17.2 TCs/year) is significantly less than during low AOD years (21.8 TCs/year). There is a tripole pattern of anomalous TC formation with fewer TCs forming over the South China Sea/Philippines and southeastern WNP but with more TCs forming over the middle part of the WNP during high AOD years compared to during low AOD years (Fig. 2b).

3.2. Changes in large-scale environmental factors

TC genesis is largely dependent on a favorable large-scale environment (Gray, 1979). We next examine how environmental factors differ between high and low AOD years to further explore the potential influence of eastern China spring AOD. In high AOD years relative to low AOD years, there is weaker 850 hPa relative vorticity and 500 hPa vertical velocity over most of the WNP, as well as stronger vertical wind shear over the southeastern part of the WNP (Fig. S1). These changes in large-scale environmental factors favor decreased WNP TCs in high AOD years and increased TCs in low AOD years. By contrast, relatively more TCs occur over the middle portion of the WNP in high AOD years relative to low AOD years, likely due to higher mid-level relative humidity in high AOD years (Fig. 3b).

The DGPI is used to further quantify the role of these large-scale factors in controlling TC frequency. As shown in Fig. 3a, the DGPI captures the observed differences in spatial TC genesis between high and low AOD years, especially over the South China Sea/Philippines region and the southeastern WNP. The relative contribution of each factor to

the DGPI is further evaluated. The total DGPI and the DGPI with varying individual factors are computed over the region where most TC genesis occurs [10°N–25°N, 110°E–180°E]. A budget analysis of the four factors suggests that 500 hPa vertical velocity plays the most important role in WNP TC differences, accounting for ~43% of the total difference (Fig. 3b). Vertical wind shear appears to be the second most important factor, accounting for ~21% of the total DGPI difference. The 500 hPa meridional gradient of the zonal wind and low-level vorticity contribute ~18% and ~14% to the total DGPI differences, respectively (Fig. 3b). Similar results can be seen when examining spatial distributions of the DGPI while varying factors in Fig. S2. 850 hPa relative vorticity, the meridional gradient of 500 hPa zonal wind and vertical wind shear all have significant areas of unfavorable conditions under higher AOD, especially in the southeastern WNP, consistent with the observed decrease in TC frequency (Fig. 2b). Relative to other factors, the DGPI terms associated with mid-tropospheric vertical velocity and vertical wind shear highlight an area favoring enhancement of TC frequency under more polluted conditions in eastern China, albeit offset to the northwest. Note that the DGPI does not reproduce well the positive TC difference over the middle portion of the WNP (Fig. 3a). This may be due to the DGPI mainly focusing on the impact of dynamic conditions on TC genesis. By contrast, thermodynamic factors, such as mid-level relative humidity, appear to play a more important role in modulating TCs over the middle portion of the WNP (Fig. S1).

4. Possible physical mechanisms

We hypothesize that aerosols over eastern China could affect the subtropical eastern Pacific circulation through SWJ transport. Consistent with increased AOD in the subtropical westerly jet (SWJ) exit region, the correlation map between spring eastern China AOD with global AOD shows a significant band over the North Pacific along the SWJ, with the two maximum centers over eastern China and the subtropical

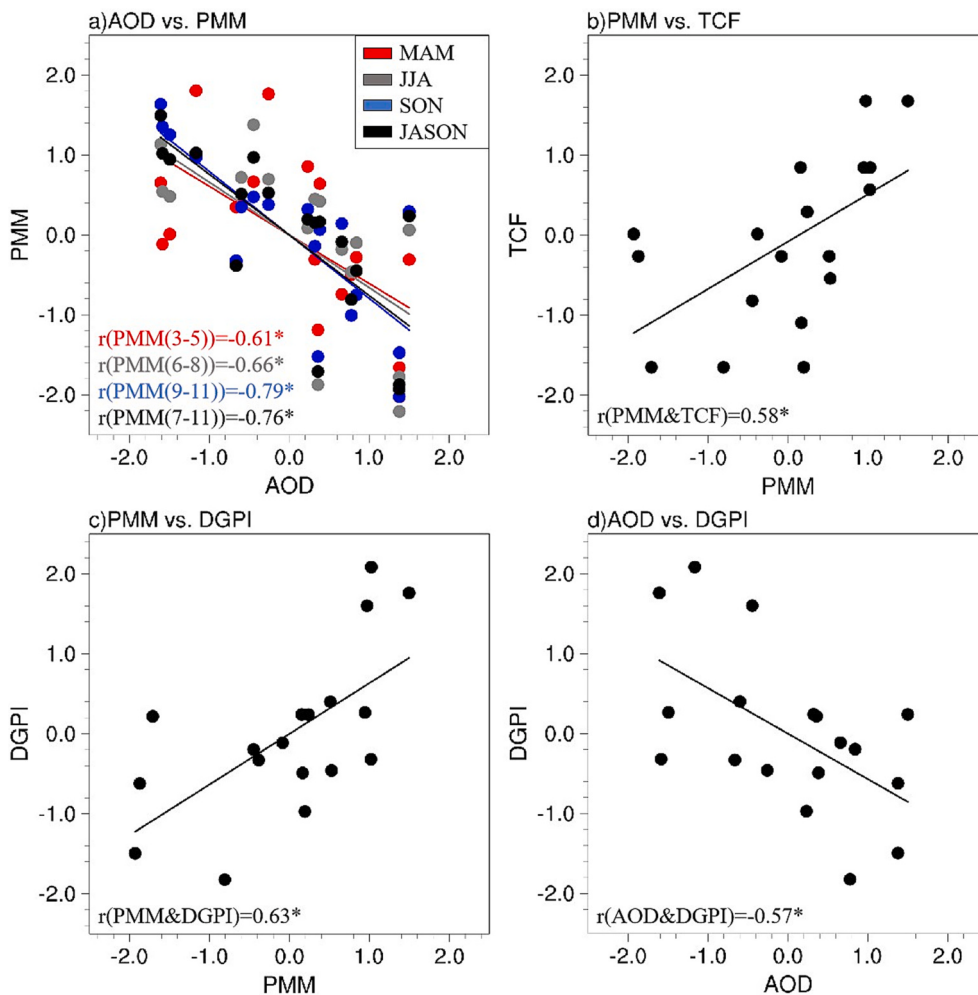


Fig. 5. (a) Standardized time series of March–May-averaged AOD over eastern China from MERRA-2 and the Pacific Meridional Mode (PMM) index for March–May, June–August, September–November and July–November during 2003–2020, (b) As in (a) but for July–November-averaged PMM index and July–November Western North Pacific TC frequency. (c) As in (a) but for July–November-averaged PMM and the July–November-averaged dynamic genesis potential index (DGPI), (d) As in (a) but for March–May-averaged eastern China AOD and July–November Western North Pacific TC frequency. Correlation coefficients that are statistically significant are denoted with an “*”.

eastern Pacific (Fig. 4a). We next examine the secondary circulation and changes in the meridional vertical temperature distribution associated with increases in aerosol loading in the SWJ exit region (Fig. 4b). Given that aerosols are mainly distributed in the middle troposphere, increased AOD would cool the lower-to-middle atmosphere, corresponding to a significant negative correlation along the northern side of the SWJ exit region (Fig. 4b). The cooling on the north side of the SWJ increases the climatological poleward negative temperature gradient, thus strengthening the SWJ and the associated secondary circulation in the SWJ exit region. Subsidence also increases on the southern side of the SWJ exit region, resulting in an anomalous low-level anticyclonic circulation (Fig. 4). The anomalous anticyclonic circulation near the North American coast further strengthens the northeasterly trades, which then cools the local subtropical eastern Pacific SST through a wind-evaporation-SST feedback, favoring the development of a negative PMM.

The robust relationship between eastern China AOD and WNP TCs may tie to the changes in decadal background SSTs. As shown in Fig. S3, positive SSTAs are located over the western North Pacific and North Atlantic and negative SSTAs are located over the eastern subtropical North Pacific during 2003–2020 compared to a 1980–2020 climatology. It agrees well with the switch of the Pacific Decadal oscillation (PDO)/Atlantic Multi-decadal oscillation (AMO) from a predominately positive/negative phase during the last part of the 20th century to a predominately negative/positive phase since the early 2000s. As suggested in prior studies (Hartmann, 2007; Kwon et al., 2010; Yu et al., 2015; Zhang and Delworth, 2007), the AMO/PDO phase change can facilitate the poleward shift of the westerly jet via momentum transport from transient vorticity and air-sea coupling processes. This highlights the

potential importance of changes in the mean SSTA state in promoting the AOD-driven negative PMM-like mode. The combined effect of the AMO and PDO as well as their respective role in contributing to the AOD-PMM-TC frequency relationship deserve further investigation.

The relationship between spring eastern China AOD and seasonal SST and low-level circulation is also examined (Fig. S4). We find significant negative correlations from the central Pacific to the North American coast during July–November, accompanied by anomalous northeasterly winds. This correlation pattern resembles a negative PMM. This relationship is further confirmed by a significant negative correlation ($r = -0.76, p < 0.05$) between March–May AOD over eastern China and the July–November PMM index (Fig. 5a). The correlations of March–May eastern China AOD with SST and 850 hPa wind from MAM to SON indicate the development and evolution of a negative PMM-like mode (Fig. S4). This PMM-like mode develops during the spring, causing anomalous cooling of SSTs over the central Pacific in subsequent seasons (MAM–SON). The negative PMM phase then forces an anomalous anticyclonic circulation over the WNP basin via a Gill-type response. Correspondingly, it is found a significant simultaneous correlation between the peak season PMM index and TC frequency over the WNP basin ($r = 0.58, p < -0.05$) (Fig. 5b). Also, there is significant association between spring eastern China AOD and PMM in subsequent seasons. The correlation between spring eastern China AOD and the PMM is -0.61 for MAM, -0.66 for JJA and -0.79 for SON, respectively (Fig. 5a). As expected, the peak season PMM index has a significant correlation with the DGPI over the main development region ($r = 0.63, p < -0.05$) (Fig. 5c). Similarly, there is a significant correlation ($r = -0.57, p < -0.05$) between spring eastern China AOD and peak season DGPI over

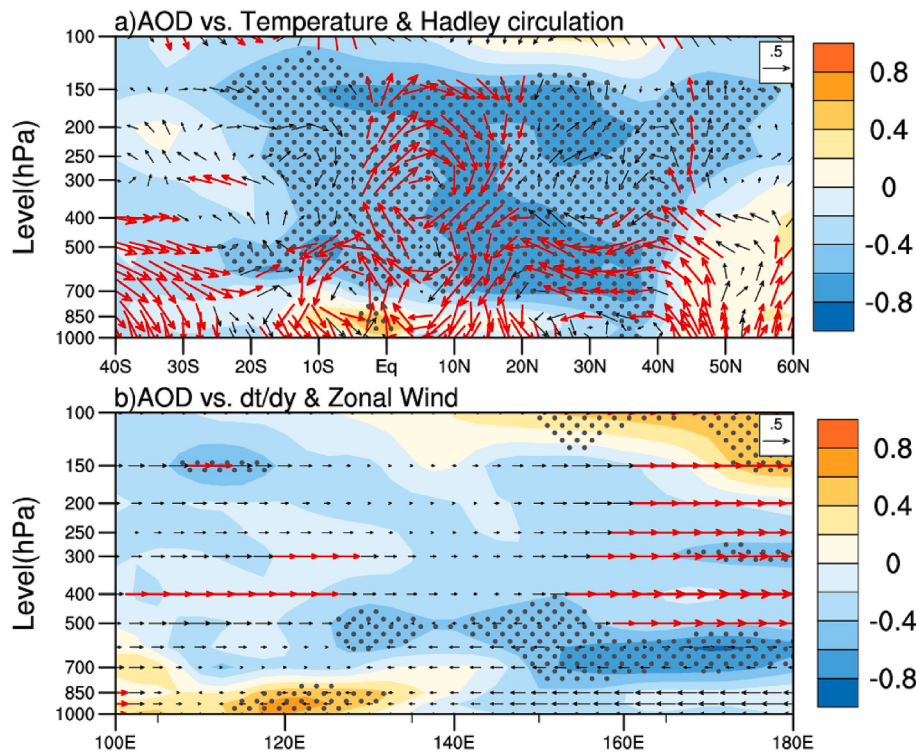


Fig. 6. (a) Pressure–latitude cross section of the correlation pattern between March–May eastern China AOD and July–November air temperature (shading), the Hadley Cell (contour) as well as wind (vectors) averaged over 110°E–180°. (b) Pressure–latitude cross section of the correlation pattern between March–May eastern China AOD and the July–November temperature gradient (shading) as well as zonal wind (vectors) averaged over 5°N–15°N. Grey dots and red vectors denote significant correlations. (For interpretation of the references to colour in this figure legend, the reader is referred to the web version of this article.)

the main development region (Fig. 5d). These results indicate that changes in spring aerosols over eastern China likely modulate TC frequency over the WNP through changes in the large-scale environment via its remote forcing of a PMM-like mode (Cai et al., 2022; Fu et al., 2023; Wang and Wang, 2019).

Changes in eastern China AOD also appear to modulate the SST gradient from equator to mid-latitude and land-sea temperature contrast, thus impacting the TC environment. As seen in the correlation map between AOD and 850-hPa wind in Fig. S4, increased AOD is associated with an anomalous anticyclonic circulation over the WNP basin and a weakened monsoon circulation. Furthermore, as shown in Fig. 6a, there is a significant negative correlation (shading) between March–May eastern China AOD and July–November Northern Hemisphere temperature. Strong anomalous cooling over the WNP associated with high eastern China AOD further reduces the interhemispheric differential, thus weakening cross-equatorial flow (Cao et al., 2022b). The anomalous low-level southward cross-equatorial flow weakens the ascending branch of the WNP Hadley circulation. Increased eastern China AOD can then increase the negative meridional temperature gradient (equator to ~20°N) (Fig. 6b), leading to westerly upper tropospheric anomalies over the southeastern WNP, thus enhancing vertical wind shear. All of these changes in the large-scale environment also disfavor WNP TCs.

5. Discussion and conclusion

This study focuses on a potential linkage between aerosol loading over eastern China and WNP TC frequency during 2003–2020. We find a significant negative relationship between eastern China AOD and WNP TC frequency during this period, meaning an increase of spring aerosol emission over eastern China being associated with a decrease of July–November WNP TC frequency. During years with larger AOD over eastern China, there is an anomalous TC tripole pattern, with a decrease of TCs over the South China Sea/Philippines and the southeastern WNP and little change in the central WNP. Changes in large-scale conditions associated with changes in eastern China AOD are largely responsible for

changes in the WNP TC genesis frequency distribution. A budget analysis of DGPI further suggests that changes in vertical motion and vertical wind shear associated with AOD anomalies appear to be the two most important dynamical factors.

Changes in large-scale factors are found to be closely associated with an AOD-driven negative PMM mode. There is a potential connection between spring aerosols over eastern China and WNP TCs via the impact of aerosols on the development of a PMM mode via the transport of the SWJ. The SWJ likely delivers more aerosols in spring during years with increased aerosol emissions over eastern China, resulting in cooling along the northern side of the SWJ exit region. During high spring AOD years, the meridional temperature gradient subsequently increases and strengthens the SWJ. This results in anomalous subsidence and an anomalous anticyclone located on the southern side of the SWJ exit region. This low-level anomalous anticyclone further cools SST through a wind-evaporation-SST feedback, favoring the development and persistence of a negative PMM phase. Via a Gill-type response, an anomalous anticyclonic circulation develops, thus inhibiting WNP TCs. Our analyses also show the potential importance of the AMO/PDO phase change in promoting the AOD-driven PMM development, the combined effect and their respective role remains unsolved in this study that deserves further investigations.

Increased AOD can also directly cool the WNP, thus decreasing the interhemispheric thermal differential, which then weakens cross-equatorial flow and the Hadley Cell. These changes then result in anomalous subsidence and anomalous low-level easterlies over the WNP. The anomalous WNP cooling due to increased AOD can increase the meridional equator to mid-latitude temperature gradient, resulting in anomalous upper-level westerlies, thus enhancing vertical wind shear over the southeastern WNP. All of these dynamic environment changes inhibit WNP TCs. TC changes over the middle portion of the WNP are not well captured by the DGPI, possibly due to the greater importance of mid-level relative humidity over this region.

The results of this study highlight the potential impact of spring eastern China AOD on WNP TC activity, improving our understanding of drivers of WNP TC variability. One caveat of this study is that this is an

observational study highlighting the relationship between eastern China AOD and WNP TCs over a relatively short study period. Further observational and modeling studies are needed to confirm these relationships.

Declaration of Competing Interest

None.

Data availability

Data will be made available on request.

Acknowledgments

This research was jointly supported by the National Key Research and Development Program of China (2022YFF0801602), the National Natural Science Foundation of China (Grant 41922033, 42005017), and the Six Talent Peaks project in Jiangsu Province (JY-100). P. Klotzbach would like to acknowledge a grant from the G. Unger Vetlesen Foundation. We acknowledge the High Performance Computing Center of Nanjing University of Information Science & Technology for their support of this work.

The data used in this manuscript are available from the following sources:

JTWC best track dataset:

<http://www.metoc.navy.mil/jtwc/jtwc.html/western-pacific>

MERRA-2, Aqua and Terra aerosol optical depth data:

<https://giovanni.gsfc.nasa.gov/giovanni/>

CAMSRA aerosol optical depth data:

<https://ads.atmosphere.copernicus.eu/>

NCEP/DOE Reanalysis II:

<https://psl.noaa.gov/data/gridded/data.ncep.reanalysis2.html>

ERSSTv5:

<https://www1.ncdc.noaa.gov/pub/data/cmb/ersst/v5/netcdf/>

PMM index:

<https://www.aos.wisc.edu/~dvimont/MModes/Data.html>

Appendix A. Supplementary data

Supplementary data to this article can be found online at <https://doi.org/10.1016/j.atmosres.2023.106604>.

References

- Cai, Y.H., Han, X., Zhao, H.K., Klotzbach, P.J., Wu, L.G., Raga, G.B., Wang, C., 2022. Enhanced predictability of rapidly intensifying tropical cyclones over the western North Pacific associated with snow depth changes over the Tibetan Plateau. *J. Clim.* 35 (7), 2093–2110. <https://doi.org/10.1175/JCLI-D-21-0758.1>.
- Camargo, S.J., Giulivi, C.F., Sobel, A.H., Wing, A.A., Kim, D., Moon, Y., Zhao, M., 2020. Characteristics of model tropical cyclone climatology and the large-Scale environment. *J. Clim.* 33 (11), 4463–4487. <https://doi.org/10.1175/JCLI-D-19-0500.1>.
- Cao, J., Wang, H., Wang, B., Zhao, H., Wang, C., Zhu, X., 2022b. Higher Sensitivity of Northern Hemisphere Monsoon to Anthropogenic Aerosol Than Greenhouse Gases. *Geophysical Research Letters* 49, e2022GL100270. <https://doi.org/10.1029/2022GL100270>.
- Cao, J., Wang, H., Zhao, H., et al., 2022a. Reversed and comparable climate impacts from historical anthropogenic aerosol and GHG on global-scale tropical cyclone genesis potential. *Environmental Research Letters* 17 (9), 094027.
- Cao, J., Zhao, H.K., Wang, B., Wu, L.G., 2021. Hemisphere-asymmetric tropical cyclones response to anthropogenic aerosol forcing. *Nat. Commun.* 12 (1), 6787. <https://doi.org/10.1038/s41467-021-27030-z>.
- Chan, J.C.L., 2008. Decadal variations of intense typhoon occurrence in the western North Pacific. *P. Roy. Soc. A Math. Phy.* 464 (2089), 249–272. <https://doi.org/10.1098/rspa.2007.0183>.
- Chan, J.C.L., Liu, K.S., 2004. Global warming and western North Pacific typhoon activity from an observational perspective. *J. Clim.* 17 (23), 4590–4602. <https://doi.org/10.1175/3240.1>.
- Chen, Q.-X., Huang, C.-L., Yuan, Y., Mao, Q.-J., Tan, H.-P., 2020. Spatiotemporal distribution of major aerosol types over China based on MODIS products between 2008 and 2017. *Atmosphere* 11 (7). <https://doi.org/10.3390/atmos11070703>.
- Chiacchio, M., Pausata, F.S.R., Messori, G., Hannachi, A., Chin, M., Onskog, T., Barrie, L., 2017. On the links between meteorological variables, aerosols, and tropical cyclone frequency in individual ocean basins. *J. Geophys. Res. Atmos.* 122 (2), 802–822. <https://doi.org/10.1002/2015JD024593>.
- Chiang, J.C.H., Vimont, D.J., 2004. Analogous Pacific and Atlantic meridional modes of tropical atmosphere–ocean variability. *J. Clim.* 17 (21), 4143–4158. <https://doi.org/10.1175/JCLI4953.1>.
- Choi, Y.-S., Ho, C.-H., Kim, J., Gong, D.-Y., Park, R.J., 2008. The impact of aerosols on the summer rainfall frequency in China. *J. Appl. Meteorol. Climatol.* 47 (6), 1802–1813. <https://doi.org/10.1175/2007JAMC1745.1>.
- Chu, J.-H., Sampson, C.R., Levine, A.S., Fukada, E., 2002. The Joint Typhoon Warning Center tropical cyclone best tracks, 1945–2000. Ref NRL/MR/7540-02 16. http://www.usno.navy.mil/NOOC/nmfc-ph/RSS/jtvc/best_tracks/TC_bt_report.html.
- Dunstone, N.J., Smith, D.M., Booth, B.B.B., Hermanson, L., Eade, R., 2013. Anthropogenic aerosol forcing of Atlantic tropical storms. *Nat. Geosci.* 6 (7), 534–539. <https://doi.org/10.1038/ngeo1854>.
- Eberenz, S., Lüthi, S., Bresch, D.N., 2021. Regional tropical cyclone impact functions for globally consistent risk assessments. *Nat. Hazards Earth Syst. Sci.* 21 (1), 393–415. <https://doi.org/10.5194/nhess-21-393-2021>.
- Emmanuel, K., Nolan, D.S., 2004. Tropical cyclone activity and the global climate system. In: *26th conference on hurricanes and tropical meteorology*.
- Fu, M., Wang, C., Wu, L., Zhao, H., 2023. Season-Dependent Modulation of Pacific Meridional Mode on Tropical Cyclone Genesis Over the Western North Pacific. *J. Geophys. Res. Atmos.* 128. <https://doi.org/10.1029/2022JD037575>.
- Gray, W.M., 1979. Tropical cyclone origin, movement and intensity characteristics based on data compositing. In: *In: techniques*, (Vol. 79, No. 6). Naval Environmental Prediction Research Facility.
- Gu, Y., Liou, K.N., Xue, Y., Mechoso, C.R., Li, W., Luo, Y., 2006. Climatic effects of different aerosol types in China simulated by the UCLA general circulation model. *J. Geophys. Res. Atmos.* 111 (D15). <https://doi.org/10.1029/2005JD006312>.
- Hartmann, D.L., 2007. The atmospheric general circulation and its variability. *J. Meteorol. Soc. Jpn., Ser. II* 85, 123–143. <https://doi.org/10.2151/jmsj.85B.123>.
- van den Heever, S.C., Carrio, G.G., Cotton, W.R., DeMott, P.J., Prenni, A.J., 2006. Impacts of nucleating aerosol on Florida storms. Part I: Mesoscale simulations. *J. Atmos. Sci.* 63 (7), 1752–1775. <https://doi.org/10.1175/JAS3713.1>.
- Huang, B.Y., Banzon, V.F., Freeman, E., Lawrimore, J., Liu, W., Peterson, T.C., Zhang, H.M., 2015. Extended reconstructed sea surface temperature version 4 (ERSST.v4). Part I: upgrades and intercomparisons. *J. Clim.* 28 (3), 911–930. <https://doi.org/10.1175/JCLI-D-14-0006.1>.
- Jenkins, G.S., Pratt, A., 2008. Saharan dust, lightning and tropical cyclones in the eastern tropical Atlantic during NAMMA-06. *Geophys. Res. Lett.* 35 (12). <https://doi.org/10.1029/2008GL033979>.
- Jenkins, G.S., Pratt, A.S., Heymsfield, A., 2008. Possible linkages between Saharan dust and tropical cyclone rain band invigoration in the eastern Atlantic during NAMMA-06. *Geophys. Res. Lett.* 35 (8). <https://doi.org/10.1029/2008GL034072>.
- Jones, A.C., Haywood, J.M., Dunstone, N., Emanuel, K., Hawcroft, M.K., Hodges, K.I., Jones, A., 2017. Impacts of hemispheric solar geoengineering on tropical cyclone frequency. *Nat. Commun.* 8. <https://doi.org/10.1038/s41467-017-01606-0>.
- Kanamitsu, M., Ebisuzaki, W., Woollen, J., Yang, S.-K., Hnilo, J.J., Fiorino, M., Potter, G.L., 2002. NCEP–DOE AMIP-II Reanalysis (R-2). *Bull. Am. Meteorol. Soc.* 83 (11), 1631–1644. <https://doi.org/10.1175/BAMS-83-11-1631>.
- Khain, A.P., 2009. Notes on state-of-the-art investigations of aerosol effects on precipitation: a critical review. *Environ. Res. Lett.* 4 (1). <https://doi.org/10.1088/1748-9326/4/1/015004>.
- Khain, A., Pokrovsky, A., Pinsky, M., Seifert, A., Phillips, V., 2004. Simulation of effects of atmospheric aerosols on deep turbulent convective clouds using a spectral microphysics mixed-phase cumulus cloud model. Part I: model description and possible applications. *J. Atmos. Sci.* 61 (24), 2963–2982. <https://doi.org/10.1175/JAS-3350.1>.
- Khain, A., Rosenfeld, D., Pokrovsky, A., 2005. Aerosol impact on the dynamics and microphysics of deep convective clouds. *Q. J. Roy. Meteor. Soc.* 131 (611), 2639–2663. <https://doi.org/10.1256/qj.04.62>.
- Khain, A.P., Benmoshe, N., Pokrovsky, A., 2008a. Factors determining the impact of aerosols on surface precipitation from clouds: an attempt at classification. *J. Atmos. Sci.* 65 (6), 1721–1748. <https://doi.org/10.1175/2007JAS251.1>.
- Khain, A., Cohen, N., Lynn, B., Pokrovsky, A., 2008b. Possible aerosol effects on lightning activity and structure of hurricanes. *J. Atmos. Sci.* 65 (12), 3652–3677. <https://doi.org/10.1175/2008JAS2678.1>.
- Khain, A.P., Leung, L.R., Lynn, B., Ghan, S., 2009. Effects of aerosols on the dynamics and microphysics of squall lines simulated by spectral bin and bulk parameterization schemes. *J. Geophys. Res. Atmos.* 114. <https://doi.org/10.1029/2009JD011902>.
- Khodri, M., Izumo, T., Vialard, J., Janicot, S., Cassou, C., Lengaigne, M., McPhaden, M.J., 2017. Tropical explosive volcanic eruptions can trigger El Niño by cooling tropical Africa (vol 8, 778, 2017). *Nat. Commun.* 8. <https://doi.org/10.1038/s41467-017-01769-w>.
- Kiehl, J.T., Briegleb, B.P., 1993. The relative roles of sulfate aerosols and greenhouse gases in climate forcing. *Science (New York, N.Y.)* 260 (5106), 311–314. <https://doi.org/10.1126/science.260.5106.311>.
- Klotzbach, P.J., Wood, K.M., Schreck III, C.J., Patricola, C.M., Bell, M.M., 2022. Trends in global tropical cyclone activity: 1990–2021. *Geophys. Res. Lett.* 49 (6). <https://doi.org/10.1029/2021GL095774>.
- Knutson, T., Camargo, S.J., Chan, J.C.L., Emanuel, K., Ho, C.-H., Kossin, J., Wu, L., 2020. Tropical cyclones and climate change assessment: Part II: projected response to anthropogenic warming. *Bull. Am. Meteorol. Soc.* 101 (3), E303–E322. <https://doi.org/10.1175/BAMS-D-18-0194.1>.

- Koren, I., Kaufman, Y.J., Rosenfeld, D., Remer, L.A., Rudich, Y., 2005. Aerosol invigoration and restructuring of Atlantic convective clouds. *Geophys. Res. Lett.* 32 (14) <https://doi.org/10.1029/2005GL023187>.
- Kwon, Y., Alexander, M.A., Bond, N.A., Frankignoul, C., Nakamura, H., Qiu, B., Thompson, L.A., 2010. Role of the Gulf Stream and Kuroshio-Oyashio Systems in Large-Scale Atmosphere–Ocean Interaction: A Review. *J. Clim.* 23 (12), 3249–3281. <https://doi.org/10.1175/2010JCLI3343.1>.
- Lee, S.S., Donner, L.J., Phillips, V.T.J., Ming, Y., 2008. The dependence of aerosol effects on clouds and precipitation on cloud-system organization, shear and stability. *J. Geophys. Res. Atmos.* 113 (D16) <https://doi.org/10.1029/2007JD009224>.
- Lee, H.S., Yamashita, T., Mishima, T., 2012. Multi-decadal variations of ENSO, the Pacific Decadal Oscillation and tropical cyclones in the western North Pacific. *Prog. Oceanogr.* 105, 67–80. <https://doi.org/10.1016/j.pocean.2012.04.009>.
- Levin, Z., Cotton, W.R., 2008. *Aerosol Pollution Impact on Precipitation: A Scientific Review*. Springer Netherlands.
- Liu, K.S., Chan, J.C.L., 2013. Inactive period of Western North Pacific Tropical Cyclone activity in 1998–2011. *J. Clim.* 26 (8), 2614–2630. <https://doi.org/10.1175/JCLI-D-12-00053.1>.
- Liu, J., Xia, X., Li, Z., Wang, P., Min, M., Hao, W., Chen, Z., 2010. Validation of multi-angle imaging spectroradiometer aerosol products in China. *Tellus, Ser. B Chem. Phys. Meteorol.* 62 (2), 117–124. <https://doi.org/10.1111/j.1600-0889.2009.00450.x>.
- Lohmann, U., Feichter, J., 2005. Global indirect aerosol effects: a review. *Atmos. Chem. Phys.* 5 (3), 715–737. <https://doi.org/10.5194/acp-5-715-2005>.
- Lynn, B.H., Khain, A.P., Dudhia, J., Rosenfeld, D., Pokrovsky, A., Seifert, A., 2005. Spectral (Bin) Microphysics Coupled with a Mesoscale Model (MMS). Part I: Model Description and First Results. *Mon. Weather Rev.* 133 (1), 44–58. <https://doi.org/10.1175/MWR-2840.1>.
- Maher, N., McGregor, S., England, M.H., Sen Gupta, A., 2015. Effects of volcanism on tropical variability. *Geophys. Res. Lett.* 42 (14), 6024–6033. <https://doi.org/10.1002/2015GL064751>.
- Mann, M.E., Emanuel, K.A., 2006. Atlantic hurricane trends linked to climate change. *EOS Trans. Am. Geophys. Union* 87 (24), 233–241. <https://doi.org/10.1029/2006EO240001>.
- McGregor, S., Timmermann, A., 2011. The effect of Explosive Tropical Volcanism on ENSO. *J. Clim.* 24 (8), 2178–2191. <https://doi.org/10.1175/2010JCLI3990.1>.
- Menon, S., 2004. Current uncertainties in assessing aerosol effects on climate. *Annu. Rev. Environ. Resour.* 29 (1), 1–30. <https://doi.org/10.1146/annurev.energy.29.063003.132549>.
- Murakami, H., Wang, B., 2022. Patterns and frequency of projected future tropical cyclone genesis are governed by dynamic effects. *Commun. Earth Environ.* 3 (1), 77. <https://doi.org/10.1038/s43247-022-00410-z>.
- Pausata, F.S.R., Camargo, S.J., 2019. Tropical cyclone activity affected by volcanically induced ITCZ shifts. *Proc. Natl. Acad. Sci. USA* 116 (16), 7732–7737. <https://doi.org/10.1073/pnas.1900771116>.
- Pausata, F.S.R., Karamperidou, C., Caballero, R., Battisti, D.S., 2016. ENSO response to high-latitude volcanic eruptions in the Northern Hemisphere: the role of the initial conditions. *Geophys. Res. Lett.* 43 (16), 8694–8702. <https://doi.org/10.1002/2016GL069575>.
- Peduzzi, P., Chatenoux, B., Dao, H., De Bono, A., Herold, C., Kossin, J., Nordbeck, O., 2012. Global trends in tropical cyclone risk. *Nat. Clim. Chang.* 2 (4), 289–294. <https://doi.org/10.1038/nclimate1410>.
- Persad, G.G., Caldeira, K., 2018. Divergent global-scale temperature effects from identical aerosols emitted in different regions. *Nat. Commun.* 9 (1), 3289. <https://doi.org/10.1038/s41467-018-05838-6>.
- Persad, G.G., Ming, Y., Shen, Z.Y., Ramaswamy, V., 2018. Spatially similar surface energy flux perturbations due to greenhouse gases and aerosols. *Nat. Commun.* 9 <https://doi.org/10.1038/s41467-018-05735-y>.
- Qian, Y., Gong, D., Fan, J., Leung, L.R., Bennartz, R., Chen, D., Wang, W., 2009. Heavy pollution suppresses light rain in China: Observations and modeling. *J. Geophys. Res. Atmos.* 114 (D7) <https://doi.org/10.1029/2008JD011575>.
- Quaas, J., Boucher, O., Bellouin, N., Kinne, S., 2008. Satellite-based estimate of the direct and indirect aerosol climate forcing. *J. Geophys. Res. Atmos.* 113 (D5) <https://doi.org/10.1029/2007JD008962>.
- Ramanathan, V., Crutzen, P.J., Kiehl, J.T., Rosenfeld, D., 2001. Aerosols, Climate, and the Hydrological Cycle. *Science* 294 (5549), 2119–2124. <https://doi.org/10.1126/science.1064034>.
- Rienecker, M.M., Suarez, M.J., Gelaro, R., Todling, R., Bacmeister, J., Liu, E., Woollen, J., 2011. MERRA: NASA's modern-era retrospective analysis for research and applications. *J. Clim.* 24 (14), 3624–3648. <https://doi.org/10.1175/JCLI-D-11-00015.1>.
- Rosenfeld, D., Lohmann, U., Raga Graciela, B., O'Dowd Colin, D., Kulmala, M., Fuzzi, S., Andreae Meinrat, O., 2008. Flood or drought: how do aerosols affect precipitation? *Science* 321 (5894), 1309–1313. <https://doi.org/10.1126/science.1160606>.
- Rosenfeld, D., Clavner, M., Nirel, R., 2011. Pollution and dust aerosols modulating tropical cyclones intensities. *Atmos. Res.* 102 (1–2), 66–76. <https://doi.org/10.1016/j.atmosres.2011.06.006>.
- Seong, M.-G., Min, S.-K., Kim, Y.-H., Zhang, X., Sun, Y., 2021. Anthropogenic greenhouse gas and aerosol contributions to extreme temperature changes during 1951–2015. *J. Clim.* 34 (3), 857–870. <https://doi.org/10.1175/JCLI-D-19-1023.1>.
- Stevens, B., Fiedler, S., Kinne, S., Peters, K., Rast, S., Musse, J., Mauritsen, T., 2017. MACv2-SP: a parameterization of anthropogenic aerosol optical properties and an associated Twomey effect for use in CMIP6. *Geosci. Model Dev.* 10 (1), 433–452. <https://doi.org/10.5194/gmd-10-433-2017>.
- Sun, Y., Zhong, Z., Li, T., Yi, L., Hu, Y., Wan, H., Li, Q., 2017. Impact of ocean warming on tropical cyclone size and its destructiveness. *Sci. Rep.-UK* 7 (1), 8154. <https://doi.org/10.1038/s41598-017-08533-6>.
- Takahashi, C., Watanabe, M., Mori, M., 2017. Significant aerosol influence on the recent decadal decrease in tropical cyclone activity over the western North Pacific. *Geophys. Res. Lett.* 44 (18), 9496–9504. <https://doi.org/10.1002/2017GL075369>.
- Thorsen, T.J., Winker, D.M., Ferrare, R.A., 2021. Uncertainty in observational estimates of the aerosol direct radiative effect and forcing. *J. Clim.* 34 (1), 195–214. <https://doi.org/10.1175/JCLI-D-19-1009.1>.
- Tie, X., Cao, J., 2009. Aerosol pollution in China: present and future impact on environment. *Particuology* 7 (6), 426–431. <https://doi.org/10.1016/j.partic.2009.09.003>.
- Tie, X., Brasseur, G.P., Zhao, C., Granier, C., Massie, S., Qin, Y., Richter, A., 2006. Chemical characterization of air pollution in eastern China and the eastern United States. *Atmos. Environ.* 40 (14), 2607–2625. <https://doi.org/10.1016/j.atmosenv.2005.11.059>.
- Wang, C., 2005. A modeling study of the response of tropical deep convection to the increase of cloud condensation nuclei concentration: 1. Dynamics and microphysics. *J. Geophys. Res. Atmos.* 110 (D21) <https://doi.org/10.1029/2004JD005720>.
- Wang, B., Murakami, H., 2020. Dynamic genesis potential index for diagnosing present-day and future global tropical cyclone genesis. *Environ. Res. Lett.* 15 (11) <https://doi.org/10.1088/1748-9326/abbb01>.
- Wang, C., Wang, B., 2019. Tropical cyclone predictability shaped by western Pacific subtropical high: integration of trans-basin sea surface temperature effects. *Clim. Dyn.* 53, 2697–2714. <https://doi.org/10.1007/s00382-019-04651-1>.
- Wang, Y., Wang, M., Zhang, R., Ghan, S.J., Lin, Y., Hu, J., Molina, M.J., 2014. Assessing the effects of anthropogenic aerosols on Pacific storm track using a multiscale global climate model. *Proc. Natl. Acad. Sci.* 111 (19), 6894–6899. <https://doi.org/10.1073/pnas.1403364111>.
- Wang, C., Wu, K., Wu, L., Zhao, H., Cao, J., 2021. What Caused the Unprecedented Absence of Western North Pacific Tropical Cyclones in July 2020? *Geophys. Res. Lett.* 48, 1–9. <https://doi.org/10.1029/2020GL092282>.
- Wu, G., Li, Z., Fu, C., Zhang, X., Zhang, R., Zhang, R., Huang, R., 2016. Advances in studying interactions between aerosols and monsoon in China. *Sci. China Earth Sci.* 59 (1), 1–16. <https://doi.org/10.1007/s11430-015-5198-z>.
- Xian, P., Klotzbach, P.J., Dunion, J.P., Janiga, M.A., Reid, J.S., Colarco, P.R., Kipling, Z., 2020. Revisiting the relationship between Atlantic dust and tropical cyclone activity using aerosol optical depth reanalyses: 2003–2018. *Atmos. Chem. Phys.* 20 (23), 15357–15378. <https://doi.org/10.5194/acp-20-15357-2020>.
- Yamaguchi, M., Chan, J.C.L., Moon, I.-J., Yoshida, K., Mizuta, R., 2020. Global warming changes tropical cyclone translation speed. *Nat. Commun.* 11 (1), 47. <https://doi.org/10.1038/s41467-019-13902-y>.
- Zhao, H., Lu, Y., Jiang, X., Klotzbach, P.J., Wu, L., Cao, J., 2022a. A Statistical Intraseasonal Prediction Model of Extended Boreal Summer Western North Pacific Tropical Cyclone Genesis. *J. Clim.* 35, 2459–2478. <https://doi.org/10.1175/JCLI-D-21-0110.1>.
- Zhao, C., Tie, X., Lin, Y., 2006. A possible positive feedback of reduction of precipitation and increase in aerosols over eastern Central China. *Geophys. Res. Lett.* 33 (11) <https://doi.org/10.1029/2006GL025959>.
- Zhao, H., Duan, X., Raga, G.B., Sun, F., 2018. Potential large-scale forcing mechanisms driving enhanced North Atlantic tropical cyclone activity since the mid-1990s. *J. Clim.* 31 (4), 1377–1397.
- Yu, L., Furevik, T., Otterå, O.H., et al., 2015. Modulation of the Pacific Decadal Oscillation on the summer precipitation over East China: a comparison of observations to 6000-year control run of Bergen Climate Model. *Clim. Dyn.* 44, 475–494. <https://doi.org/10.1007/s00382-014-2141-5>.
- Zhang, R., Delworth, T.L., 2007. Impact of the Atlantic Multidecadal Oscillation on North Pacific climate variability. *Geophys. Res. Lett.* 34, L23708. <https://doi.org/10.1029/2007GL031601>.
- Zhao, H., Chen, S., Raga, G.B., Phil, J., Klotzbach, P.J., Wu, L., 2019. Recent decrease in genesis productivity of tropical cloud cluster over the western North Pacific. *Clim. Dyn.* 52, 5819–5831.
- Zhao, H.K., Zhao, K., Cao, J., Klotzbach, P.J., Raga, G.B., Ma, Z.H., 2021a. Meridional migration of eastern North Pacific tropical cyclogenesis: Joint contribution of interhemispheric temperature differential and ENSO. *J. Geophys. Res. Atmos.* 126 (10) <https://doi.org/10.1029/2020JD034504>.
- Zhao, H., Zhao, K., Klotzbach, P.J., Liguang, W.U., Wang, C., 2022b. Interannual and Interdecadal Drivers of Meridional Migration of Western North Pacific Tropical Cyclone Lifetime Maximum Intensity Location. *J. Clim.* 35, 2709–2722. <https://doi.org/10.1175/JCLI-D-21-0797.1>.
- Zhao, K., Zhao, H., Raga, G.B., et al., 2021b. Changes in extended boreal summer tropical cyclogenesis associated with large-scale flow patterns over the western North Pacific in response to the global warming hiatus. *Clim. Dyn.* 56 (1), 515–535.